Journal of Applied Physics

Tuning energy barriers by doping 2D group-IV monochalcogenides

Cite as: J. Appl. Phys. **127**, 234103 (2020); https://doi.org/10.1063/5.0008502
Submitted: 23 March 2020 • Accepted: 02 June 2020 • Published Online: 17 June 2020

Albert Du, Zachary Pendergrast and Salvador Barraza-Lopez

Journal of Applied Physics ARTICLE scitation.org/journal/jap

Tuning energy barriers by doping 2D group-IV monochalcogenides

Cite as: J. Appl. Phys. **127**, 234103 (2020); doi: 10.1063/5.0008502
Submitted: 23 March 2020 · Accepted: 2 June 2020 ·
Published Online: 17 June 2020

Albert Du, Zachary Pendergrast, and Salvador Barraza-Lopez[a)]

AFFILIATIONS

Department of Physics, University of Arkansas, Fayetteville, Arkansas 72701, USA

Note: This paper is part of the Special Topic on: Beyond Graphene: Low Symmetry and Anisotropic 2D Materials.
[a)]**Author to whom correspondence should be addressed:** sbarraza@uark.edu

ABSTRACT

Structural degeneracies underpin the ferroic behavior of anisotropic next-generation two-dimensional materials and lead to peculiar two-dimensional structural transformations under external fields, charge doping, and/or temperature. The most direct indicator of the ease of these transformations is an *elastic energy barrier*, defined as the energy difference between the (degenerate) structural ground state unit cell and a unit cell with an increased structural symmetry. Proximity of a two-dimensional material to a bulk substrate can affect the magnitude of the critical fields and/or temperature at which these transformations occur, with the first effect being a relative charge transfer, which could trigger a structural quantum phase transition. With this physical picture in mind, we report the effect of modest charge doping (within -0.2 and $+0.2$ electrons per unit cell) on the elastic energy barrier J_s of ferroelastic black phosphorene and nine ferroelectric/ferroelastic monochalcogenide monolayers. J_s is the energy needed to create a $Pnm2_1 \rightarrow P4/nmm$ two-dimensional structural transformation, and it is sensitive to the orbital character of the electronic charge added or removed. Similar to the effect on the elastic energy barrier of ferroelastic SnO monolayers, group-IV monochalcogenide monolayers show a tunable elastic energy barrier for similar amounts of doping, and a decrease (increase) of J_s can be engineered under a modest hole (electron) doping of not more than one-tenth of an electron or a hole per atom.

I. INTRODUCTION

In the very recent past, Zhu *et al.* have shown that the intrinsic electric dipole of SnSe monolayers can be tuned by charge doping.[1] Charge doping is a variant of charge density reaccommodation, with another instance of electronic rearrangement, dipole screening, and structural modifications being created by illumination from light.[2] Reference 1 employed the Perdew–Burke–Ernzerhof (PBE) approximation for exchange and correlation[3] in density functional theory.[4]

According to Seixas *et al.*[5] and others,[6,7] charge doping also modifies energy barriers separating the ground state ferroelectric unit cell and paraelectric unit cells that have an enhanced symmetry. As indicated by Potts,[8] a change in energy barriers in turn modifies the critical temperature at which structural phase transformations take place in ferroic 2D materials. Thus far, only chemical composition,[9,10] strain,[11] and structural constraints[12] have been studied as means to control energy barriers of group-IV monochalcogenides, and this manuscript shows that energy barriers are also susceptible of change upon charge doping, which could occur by proximity to a supporting substrate.[13–16]

In doing so, we recall that density functional theory methods are unable to describe the electron correlation in so-called "van der Waals solids" accurately, as explicitly shown in the bulk and in bilayers of black phosphorus.[17] One may conclude that this may also be the case for isoelectronic group-IV monochalcogenide monolayers. Previous work from us[10] questions the accuracy of exchange-correlation approximations, such as local-density approximation (LDA)[18,19] or even PBE,[3] and suggests that these materials could become a testbed for further work in exchange-correlation functionals. In that previous study, geometries were determined from density functional theory[4] using eight different exchange-correlation (XC) functionals that include traditional ones (LDA[18,19] and PBE[3]), five with self-consistent van der Waals corrections[20–22] (vdW-DF-optPBE,[23,24] vdW-DF-optB86b,[23,24] vdW-DF-cx,[25] vdW-DF2-rPW86,[26] and vdW-DF2-B86R[26,27]), and the recently developed SCAN+rVV10,[28] which has been successful to describe the weak bonding in liquid and solid water in the most precise manner yet.[29] In order to test the predictions obtained with the PBE exchange-correlation functional, we worked with the

vdW-DF2-B86R[26,27] and with a combination of optPBE exchange and DF2 correlation corrections (vdW-DF2-optPBE) here; these choices were made for purely illustrative purposes only.

The atomistic structure of black phosphorus monolayers and most group-IV monochalcogenide monolayers is peculiar in that a finite horizontal tilt $\delta_{x,0}$ (or d in Ref. 1) exists in between pairs of atoms (exceptions are PbS, PbSe, and PbTe for which $\delta_{x,0} = 0$[9,10]). Additional variables that permit understanding the structural evolution with charge doping are lattice parameters $a_{1,0}$ and $a_{2,0}$[9–12] (labeled a and b in Ref. 1). The angle α in Ref. 1 is not a good descriptor of a paraelectric structure.

The process to obtain energy barriers under doping is straightforward, but additional steps beyond those described in Ref. 1 are necessary. The main difference is that while the focus of Ref. 1 is on the ground state unit cell which has a $Pnm2_1$ symmetry,[30] the barrier J_s to be calculated here is the energy difference among such ground state unit cell and a paraelectric unit cell with P4/nmm symmetry.

The manuscript is straightforward, it has a decisive emphasis on atomistic structure, and is organized as follows: Computational details are provided in Sec. II, a comparative discussion that includes the results from Zhu and co-workers obtained with the PBE approximation to exchange correlation and ours, and the calculation of energy barriers is provided in Sec. III. Conclusions are provided in Sec. IV.

II. COMPUTATIONAL DETAILS

Calculations were performed with the VASP code[31] (release 5.4.4) on a $30 \times 30 \times 1$ k-point mesh and with a 600 eV energy cutoff. Energy and force convergence criteria were set to 10^{-11} eV and 10^{-5} eV/Å, respectively, and the high precision tag was turned on. The out-of-plane lattice vector length was 30 Å. The anharmonicity of the energy landscape of monolayers makes it difficult for standard algorithms that optimize lattice vectors to find the overall minima. We have, therefore, performed calculations on pre-established lattice parameter meshes (i.e., in meshes for which the variation of energy against lattice parameters is sampled with a 0.005 Å resolution and the four basis atoms are allowed to move along the x- and z-directions).

III. RESULTS AND DISCUSSION

Figure 1 shows the evolution of zero-temperature $\delta_{x,0}$ vs charge doping; the inset of Fig. 1(a) showing its schematic depiction. In the inset, the four atoms forming the unit cell are shown; the gray atom

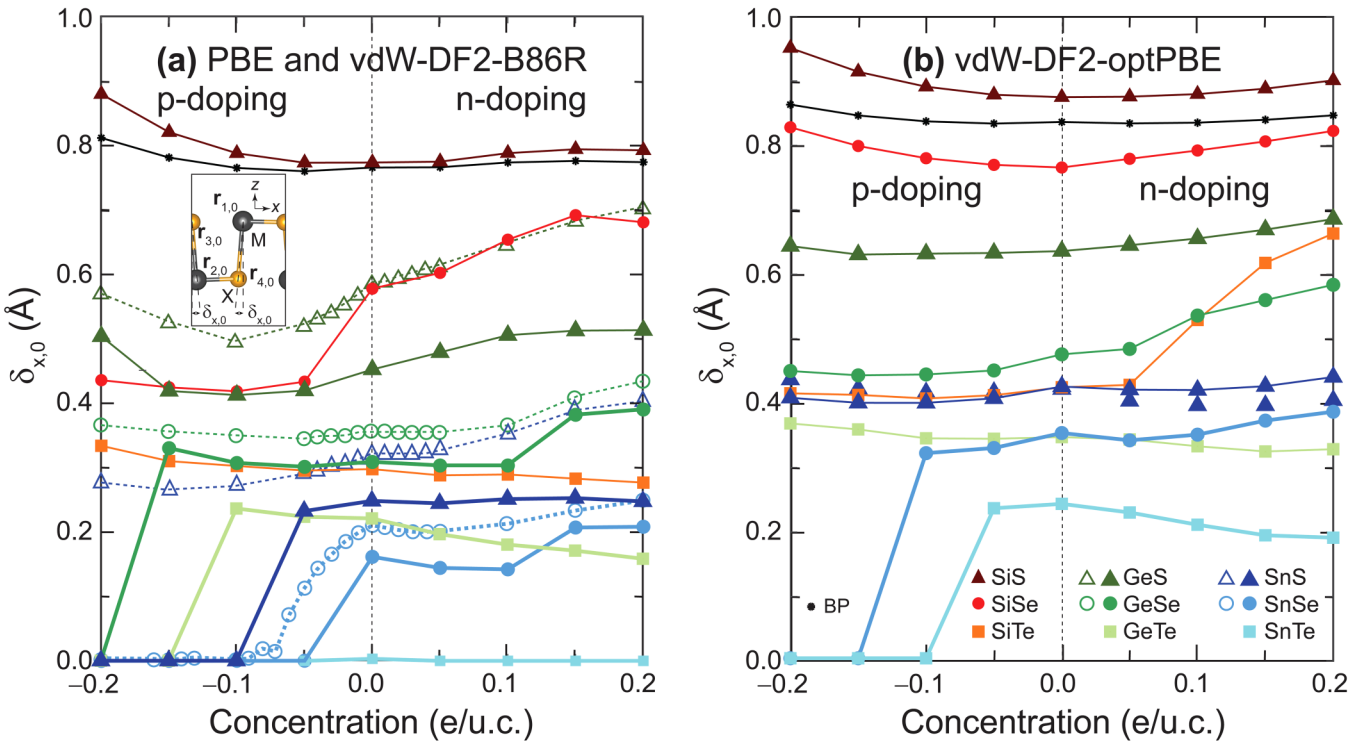

FIG. 1. Order parameter $\delta_{1,0}$ as a function of hole/electron concentration for the black phosphorus monolayer and nine group-IV monochalcogenide monolayers (SiS, SiSe, SiTe, GeS, GeSe, GeTe, SnS, SnSe, and SnTe). (a) Results with the vdW-DF2-B86R exchange-correlation functional are shown in solid symbols, and PBE results from Ref. 1 can be seen as open symbols. GeSe, GeTe, SnS, SnSe, and SnTe monolayers are paraelectric with a modest hole doping of 0.2 holes/u.c. (b) As the alternate calculation employing the vdW-DF2-optPBE functional shows, the magnitude of $\delta_{x,0}$ is strongly dependent on exchange-correlation functional: here, SnSe and SnTe monolayers become paraelectric under a doping of 0.2 holes/u.c.

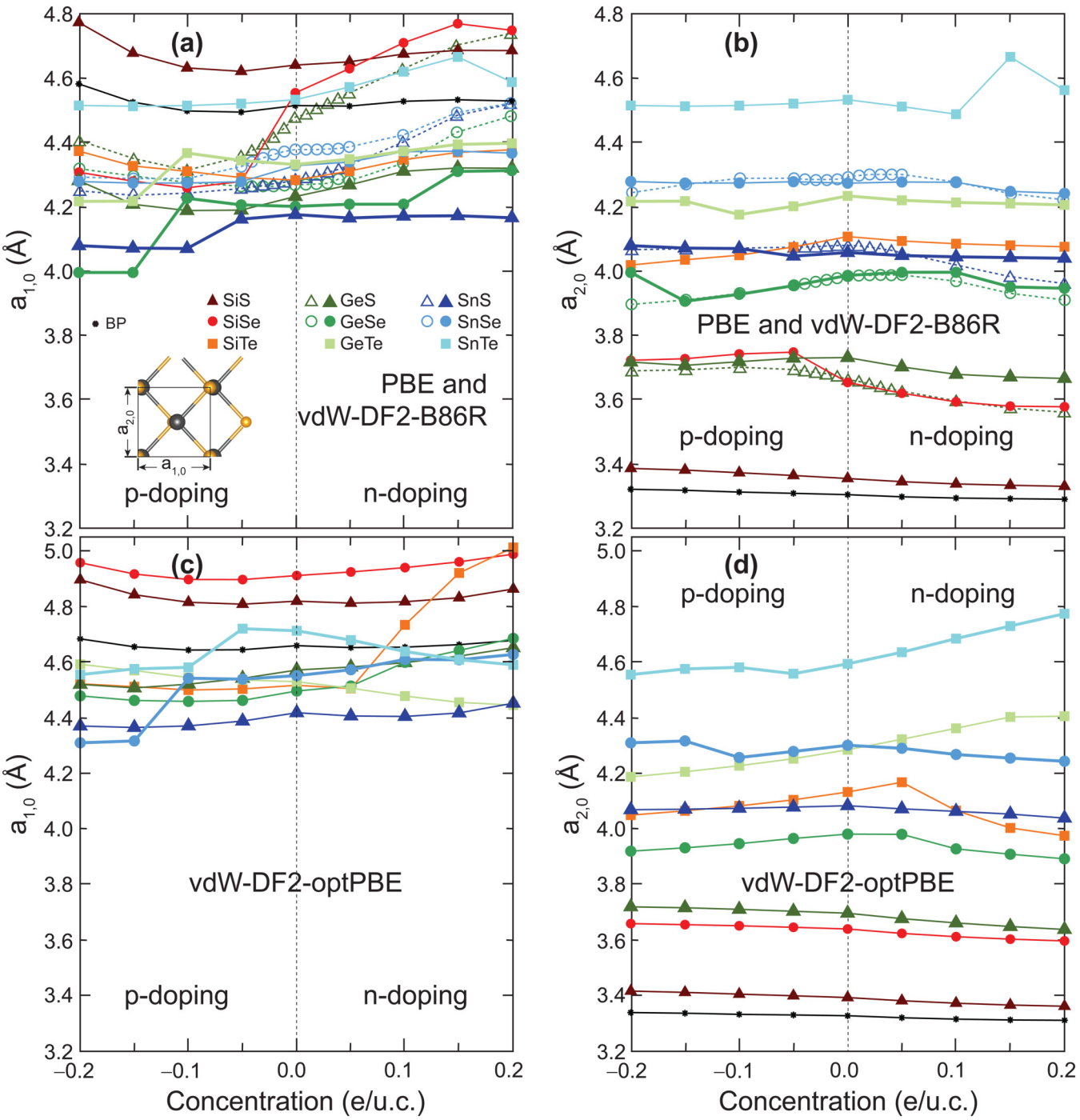

FIG. 2. Lattice parameters $a_{1,0}$ [subplots (a) and (c)] and $a_{2,0}$ [subplots (c) and (d)] as a function of charge doping concentration. Results in subplots (a) and (b) were obtained with the vdW-DF2-B86R exchange-correlation functional, and open symbols correspond to calculations with the PBE exchange correlation functional in Ref. 1. Note that heavier monochalcogenide monolayers (GeSe, GeTe, SnS, SnSe, and SnTe) have identical lattice parameters for the largest shown hold doping. Subplots (c) and (d) show data obtained with the vdW-DF2-optPBE exchange-correlation functional. In this case, only SnSe and SnTe monolayer show converging lattice parameters for the largest hole doping shown in these subplots.

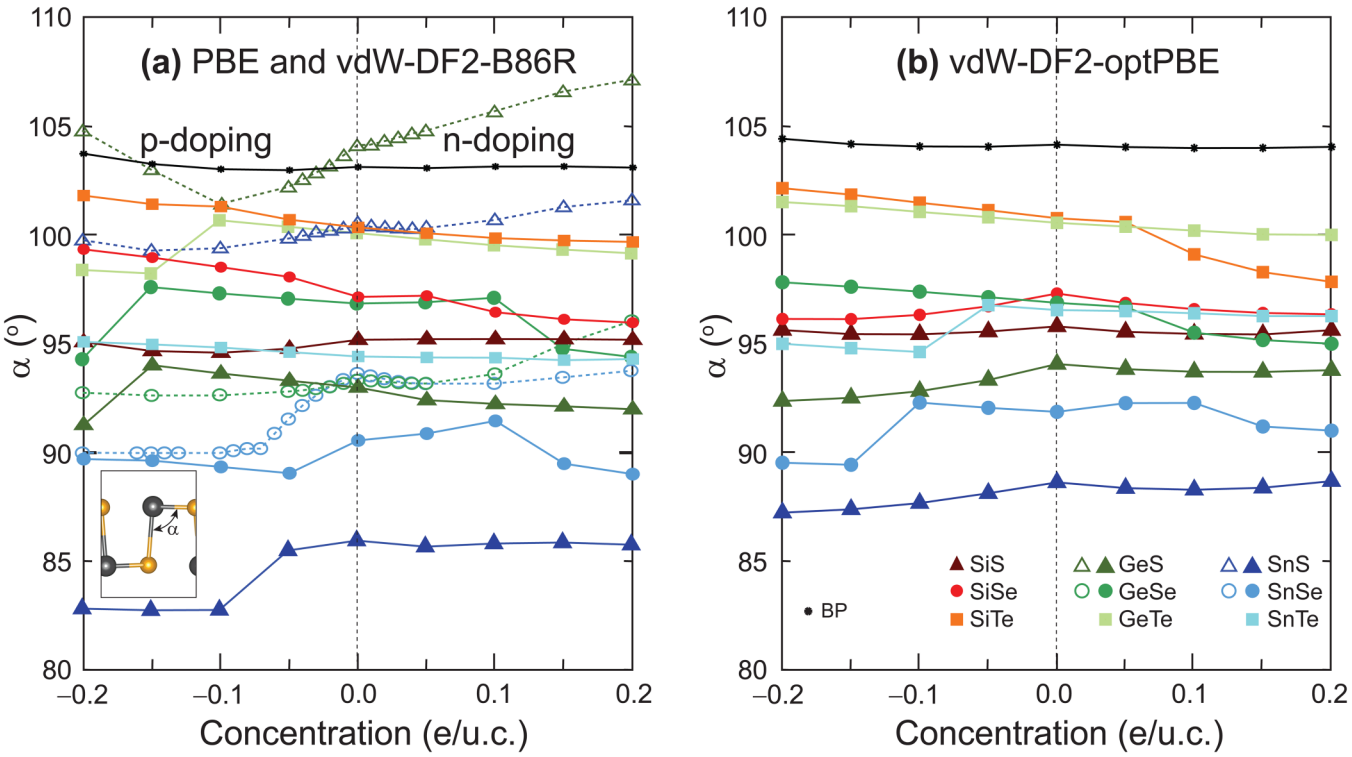

FIG. 3. The angle α is not a reliable order parameter of a paraelectric u.c. as a function of charge doping: its magnitude does not necessarily correlate with $\delta_{x,0} = 0$ in Fig. 1. Furthermore, α can take smaller or larger values than 90°. (a) Results with the vdW-DF2-B86R exchange-correlation functional are shown in solid symbols, and PBE results from Ref. 1 can be seen as open symbols. (b) Alternative calculation employing the vdW-DF2-optPBE exchange-correlation functional.

is the group-IV (metal, M) element and the yellow one the chalcogen (X).

The vdW-DF2-B86R functional in Fig. 1(a) performs in a manner analog to PBE in the four materials (GeS, GeSe, SnS, and SnSe) studied previously[1] (shown in dashed lines and open symbols). We can attest to the accuracy of the charge-neutral structures in Ref. 1, as our PRB results are spot-on[10] when compared with theirs.

The vdW-DF2-B86R exchange-correlation functional provides a structure slightly compressed with respect to PBE, as will be seen more clearly in Fig. 2 when lattice parameters are revealed. Results with the vdW-DF2-B86R functional provide slightly *smaller* magnitudes of $\delta_{x,0}$ when compared to previous PBE results. Additionally, there is a salient difference in our results and previous ones: while we confirm that SnSe monolayers are paraelectric under hole doping, *we also observe SnTe, SnS, GeTe, and even GeSe to turn paraelectric under hole doping* (previous work does not report GeSe, GeTe, nor SnS to be paraelectric). Occurring at zero temperature, *the change from a ferroelectric to a paraelectric ground state structure upon doping is a quantum phase transition.*[32]

As seen in Fig. 1(b), the magnitude of $\delta_{x,0}$ obtained when employing the vdW-DF2-optPBE functional is larger than that observed with PBE or vdW-DF2-B86R. This is due to the variation in the structure observed among many exchange-correlation functionals as reported in Ref. 10. The larger magnitude of $\delta_{x,0}$ is such that only SnSe and SnTe monolayers can become paraelectric under the amount of charge doping shown in the figure.

We now turn our attention to the evolution of zero-temperature lattice parameters $a_{1,0}$ and $a_{2,0}$ as a function of charge doping for black phosphorus and the nine group-IV monochalcogenide monolayers. For this purpose, the left subplots in Fig. 2 display $a_{1,0}$, while subplots to the right show $a_{2,0}$. Once again, it is possible to see the close correspondence among vdW-DF2-B86R and PBE results, and the larger values (especially of $a_{1,0}$ when the vdW-DF2-optPBE exchange correlation functional is employed. We chose to give an identical range for both lattice parameters in order to emphasize that they can take on identical values for those cases in which $\delta_{x,0}$ turned zero in Fig. 1.

The angle α in Ref. 1 is formed among atoms $\mathbf{r}_{3,0}$, $\mathbf{r}_{2,0}$, and $\mathbf{r}_{4,0}$ at the inset of Fig. 1(a). Using their atomic positions as defined before,[10,11]

$$\mathbf{r}_{3,0} = (0, 0, z_{3,0}), \quad \mathbf{r}_{2,0} = (\delta_{x,0}, 0, 0), \quad \text{and}$$
$$\mathbf{r}_{4,0} = \left(\frac{a_{1,0}}{2}, \frac{a_{2,0}}{2}, z_{z,0} - z_{3,0}\right),$$

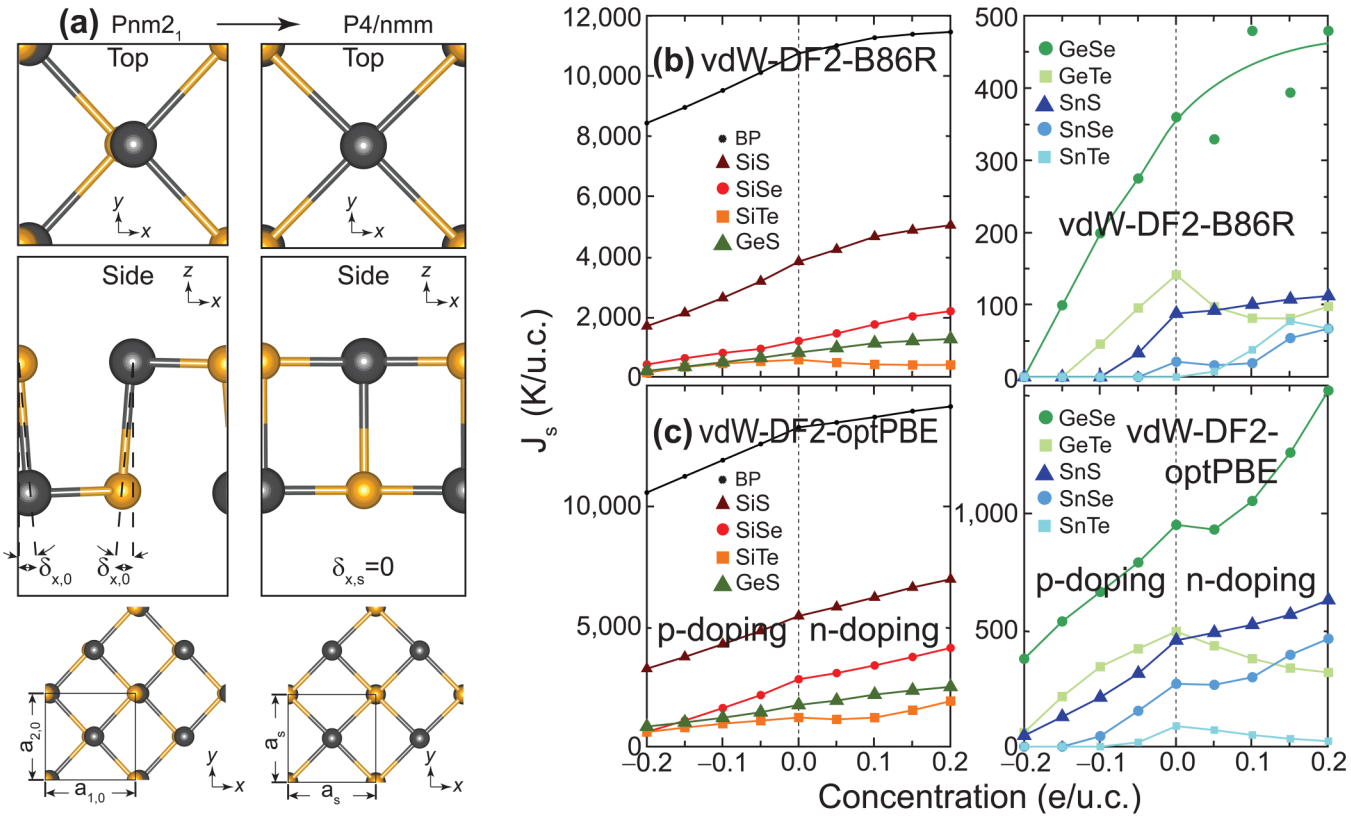

FIG. 4. (a) Geometrical depiction of the Pnm2$_1$ → P4/nmm structural transformation, leading to the barrier J_s. (b) Energy barriers J_s as obtained for the vdW-DF2-B86R exchange correlation functional. (c) Energy barriers J_s as obtained for the vdW-DF2-optPBE exchange correlation functional. There is a clear decrease (increase) of J_s with hole (electron) doping.

with $z_{1,0}$ and $z_{3,0}$ relative heights with respect to atom $\mathbf{r}_{2,0}$ (which is placed at a zero height), it becomes possible to write down a compact expression, as follows:

$$\cos\alpha = \frac{-\delta_{x,0}\left(\frac{a_{1,0}}{2}-\delta_{x,0}\right)+z_{3,0}(z_{1,0}-z_{3,0})}{\sqrt{\delta_{x,0}^2+z_{3,0}^2}\sqrt{\left(\frac{a_{1,0}}{2}-\delta_{x,0}\right)^2+\left(\frac{a_{2,0}}{2}\right)^2+(z_{1,0}-z_{3,0})^2}}. \quad (1)$$

Equation (1) gives important information away. The first term in its numerator is smaller or equal than zero, as $0 \leq \delta_{x,0} < a_{1,0}$. In turn, the second term in its numerator is larger or equal than zero. In particular, and as indicated as early as 2016, the relative height of the lowermost atoms $z_{1,0} - z_{3,0}$ *can be negative or positive depending on the chemical compound,*[33] while it appears that Ref. 1 assumes it to be zero (as that would be the only way $\alpha \geq 90^\circ$ in that work). In other words, and as seen in Fig. 3, α should not be employed as the order parameter to signal the ferroelectric to paraelectric quantum phase transformation.

It is time to shift gears and show how the elastic energy barrier J_s is influenced by charge doping. For this purpose, Fig. 4(a) displays the ferroelectric orthorhombic ground state unit cell with Pnm2$_1$ group symmetry, and the paraelectric tetrahedral unit cell with P4/nmm group symmetry from which J_s is computed.[9,10] The units of J_s (K/u.c.) are directly proportional to the critical temperature T_c at which the structural transformation takes place.[12] Figures 4(b) and 4(c) show that the barrier is smaller with hole doping, and it gradually increases to take largest values with electron doping, for a certain degree of tunability.

The enhancement of J_s with electron doping (n-doping) in Fig. 4 is due to the fact that the conduction band edge has a strong px orbital character, resulting in a larger tilt $\delta_{x,0}$ and an elongation of the unit cell along the x-direction (Figs. 1 and 2) when these orbitals get populated (Ref. 2). In contrast, hole doping (p-doping) results in a less asymmetric charge density distribution, favoring a less rectangular unit cell and a smaller J_s. Due to the largest magnitudes of both $\delta_{x,0}$ and $a_{1,0}$ reported in Figs. 1 and 2, the barrier is larger when employing the vdW-DF2-optPBE functional. As indicated before, J_s is the first estimate of a possible critical temperature at which the ferroelectric to paraelectric structural transformation might take place,[9,12] and hence the significance of the tunability observed in Fig. 4. The fact that the barriers increase in going from hole to electron doping give confidence that such phenomena may

be independent of the exchange-correlation functional being employed and is thus a reliable feature of these materials.

IV. CONCLUSIONS

To conclude, we studied the effect of charge doping (within −0.2 to +0.2 electrons per unit cell) on the elastic energy barrier J_s created by a $Pnm2_1 \rightarrow P4/nmm$ two-dimensional structural transformation of ferroelastic black phosphorene and nine ferroelectric monochalcogenide monolayers, using vdW-DF2-B86R and vdW-DF2-optPBE exchange-correlation functionals for this purpose. These barriers are crucial to determine the structural transformation. The effect of charge doping on these barriers we had never assessed before.

Providing a comparison against recent results published in this journal, the zero-temperature evolution of the in-plane tilt $\delta_{x,0}$, an angle α, and lattice parameters $a_{1,0}$ and $a_{2,0}$ of the ground state unit cell were also studied along the way.

Group-IV monochalcogenide monolayers show a tunable elastic energy barrier for similar amounts of doping: a decrease (increase) of J_s can be engineered under a modest hole (electron) doping of no more than one-tenth of an electron or a hole per atom. These results provide further guidance concerning a possible tunability of the critical temperature of these compounds by charge doping.

ACKNOWLEDGMENTS

A.D. was funded by the NSF through a Research Experience for Undergraduates (REU) program at the University of Arkansas, Grant No. DMR-1851919. Z.P. received support from National Science Foundation (NSF), Grant No. DMR-1610126. S.B.-L. was funded by an Early Career Grant from the DOE (Award DE-SC0016139). Calculations were performed on Cori at NERSC, a U.S. DOE Office of Science User Facility operated under Contract No. DE-AC02-05CH11231, and on Trestles and Pinnacle at Arkansas, funded by the U.S. National Science Foundation (Grant Nos. 0722625, 0959124, 0963249, and 0918970), a grant from the Arkansas Economic Development Commission, and the Office of the Vice Provost for Research and Innovation.

DATA AVAILABILITY

The data that support the findings of this study are available from the corresponding author upon reasonable request.

REFERENCES

[1]L. Zhu, Y. Lu, and L. Wang, "Tuning ferroelectricity by charge doping in two-dimensional SnSe," J. Appl. Phys. **127**, 014101 (2020).
[2]R. Haleoot, C. Paillard, T. P. Kaloni, M. Mehboudi, B. Xu, L. Bellaiche, and S. Barraza-Lopez, "Photostrictive two-dimensional materials in the monochalcogenide family," Phys. Rev. Lett. **118**, 227401 (2017).
[3]J. P. Perdew, K. Burke, and M. Ernzerhof, "Generalized gradient approximation made simple," Phys. Rev. Lett. **77**, 3865–3868 (1996).
[4]R. M. Martin, *Electronic Structure: Basic Theory and Practical Methods* (Cambridge University Press, Cambridge, UK, 2004).
[5]L. Seixas, A. S. Rodin, A. Carvalho, and A. H. Castro Neto, "Multiferroic two-dimensional materials," Phys. Rev. Lett. **116**, 206803 (2016).
[6]T. B. Bishop, E. E. Farmer, A. Sharmin, A. Pacheco-Sanjuan, P. Darancet, and S. Barraza-Lopez, "Quantum paraelastic two-dimensional materials," Phys. Rev. Lett. **122**, 015703 (2019).
[7]S. Barraza-Lopez, "Toward quantum paraelectric, paraelastic, and paramagnetic 2d materials," Ann. Phys. **532**, 1900448 (2020).
[8]R. B. Potts, "Some generalized order-disorder transformations," Math. Proc. Cambridge Philos. Soc. **48**, 106 (1952).
[9]M. Mehboudi, A. M. Dorio, W. Zhu, A. van der Zande, H. O. H. Churchill, A. A. Pacheco-Sanjuan, E. O. Harriss, P. Kumar, and S. Barraza-Lopez, "Two-dimensional disorder in black phosphorus and monochalcogenide monolayers," Nano Lett. **16**, 1704–1712 (2016).
[10]S. P. Poudel, J. W. Villanova, and S. Barraza-Lopez, "Group-IV monochalcogenide monolayers: Two-dimensional ferroelectrics with weak intralayer bonds and a phosphorenelike monolayer dissociation energy," Phys. Rev. Mater. **3**, 124004 (2019).
[11]S. Barraza-Lopez, T. P. Kaloni, S. P. Poudel, and P. Kumar, "Tuning the ferroelectric-to-paraelectric transition temperature and dipole orientation of group-IV monochalcogenide monolayers," Phys. Rev. B **97**, 024110 (2018).
[12]J. W. Villanova, P. Kumar, and S. Barraza-Lopez, "Theory of finite-temperature two-dimensional structural transformations in group-IV monochalcogenide monolayers," Phys. Rev. B **101**, 184101 (2020).
[13]K. Chang, J. Liu, H. Lin, N. Wang, K. Zhao, A. Zhang, F. Jin, Y. Zhong, X. Hu, W. Duan, Q. Zhang, L. Fu, Q.-K. Xue, X. Chen, and S.-H. Ji, "Discovery of robust in-plane ferroelectricity in atomic-thick SnTe," Science **353**, 274–278 (2016).
[14]K. Chang, B. J. Miller, H. Yang, H. Lin, S. S. P. Parkin, S. Barraza-Lopez, Q.-K. Xue, X. Chen, and S.-H. Ji, "Standing waves induced by valley-mismatched domains in ferroelectric SnTe monolayers," Phys. Rev. Lett. **122**, 206402 (2019).
[15]K. Chang, T. P. Kaloni, H. Lin, A. Bedoya-Pinto, A. K. Pandeya, I. Kostanovskiy, K. Zhao, Y. Zhong, X. Hu, Q.-K. X. Xue, X. Chen, S.-H. Ji, S. Barraza-Lopez, and S. S. P. Parkin, "Enhanced spontaneous polarization in ultrathin SnTe films with layered antipolar structure," Adv. Mat. **31**, 1804428 (2019).
[16]T. P. Kaloni, K. Chang, B. J. Miller, Q.-K. Xue, X. Chen, S.-H. Ji, S. S. P. Parkin, and S. Barraza-Lopez, "From an atomic layer to the bulk: Low-temperature atomistic structure and ferroelectric and electronic properties of SnTe films," Phys. Rev. B **99**, 134108 (2019).
[17]L. Shulenburger, A. D. Baczewski, Z. Zhu, J. Guan, and D. Tománek, "The nature of the interlayer interaction in bulk and few-layer phosphorus," Nano Lett. **15**, 8170 (2015).
[18]D. M. Ceperley and B. J. Alder, "Ground state of the electron gas by a stochastic method," Phys. Rev. Lett. **45**, 566–569 (1980).
[19]J. P. Perdew and A. Zunger, "Self-interaction correction to density-functional approximations for many-electron systems," Phys. Rev. B **23**, 5048–5079 (1981).
[20]A. D. Becke, "On the large–gradient behavior of the density functional exchange energy," J. Chem. Phys. **85**, 7184–7187 (1986).
[21]M. Dion, H. Rydberg, E. Schröder, D. C. Langreth, and B. I. Lundqvist, "Van der Waals density functional for general geometries," Phys. Rev. Lett. **92**, 246401 (2004).
[22]K. Berland, V. R. Cooper, K. Lee, E. Schröder, T. Thonhauser, P. Hyldgaard, and B. I. Lundqvist, "Van der Waals forces in density functional theory: A review of the vdW-DF method," Rep. Prog. Phys. **78**, 066501 (2015).
[23]J. Klimeš, D. Bowler, and A. Michaelides, "Chemical accuracy for the van der Waals density functional," J. Phys. Condens. Matter. **22**, 022201 (2010).
[24]J. Klimeš, D. Bowler, and A. Michaelides, "Van der Waals density functionals applied to solids," Phys. Rev. B **83**, 195131 (2011).
[25]K. Berland and P. Hyldgaard, "Exchange functional that tests the robustness of the plasmon description of the van der Waals density functional," Phys. Rev. B **89**, 035412 (2014).
[26]K. Lee, E. D. Murray, L. Kong, B. I. Lundqvist, and D. C. Langreth, "Higher-accuracy van der Waals density functional," Phys. Rev. B **82**, 081101 (2010).

[27]I. Hamada, "Van der Waals density functional made accurate," Phys. Rev. B **89**, 121103 (2014).
[28]H. Peng, Z.-H. Yang, J. P. Perdew, and J. Sun, "Versatile van der Waals density functional based on a meta-generalized gradient approximation," Phys. Rev. X **6**, 041005 (2016).
[29]M. Chen, H.-Y. Ko, R. C. Remsing, M. F. Calegari Andrade, B. Santra, Z. Sun, A. Selloni, R. Car, M. L. Klein, J. P. Perdew, and X. Wu, "*Ab initio* theory and modeling of water," Proc. Natl. Acad. Sci. **114**, 10846–10851 (2017).
[30]A. S. Rodin, L. C. Gomes, A. Carvalho, and A. H. Castro Neto, "Valley physics in tin (II) sulfide," Phys. Rev. B **93**, 045431 (2016).
[31]G. Kresse and J. Furthmüller, "Efficient iterative schemes for *ab initio* total-energy calculations using a plane-wave basis set," Phys. Rev. B **54**, 11169–11186 (1996).
[32]S. Sachdev, *Quantum Phase Transitions* (Cambridge University Press, Cambridge, UK, 2011).
[33]C. Kamal, A. Chakrabarti, and M. Ezawa, "Direct band gaps in group IV-VI monolayer materials: Binary counterparts of phosphorene," Phys. Rev. B **93**, 125428 (2016).